# Newly Developed Wavefront Metrology Technique and Applying in Crystal Processing

**Fang Liu**, Zhen Hong, Ming Li, Junliang Yang, Qianshun Diao, Zhe Li, Hongkai Lian, Changrui Zhang
Institute of High Energy Physics
2023-11-07

# Outline

# Wavefront Metrology Technique

- **The double-edge scan method (DES)**
  - Background
  - Method introduction

# Background

➢ **Challenges that the crystals faced (processing & wavefront measurement)**

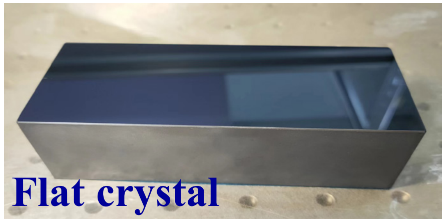


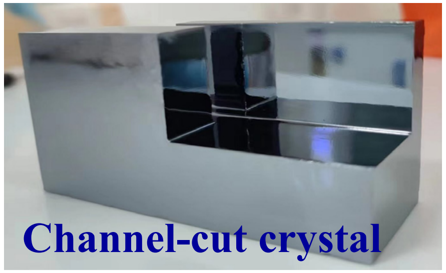


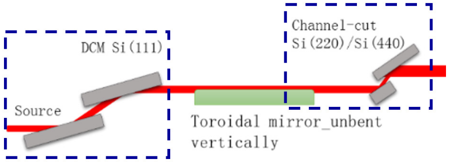


Crystal monochromators are widely used in beamlines.



Transverse coherence：
~0.2% -> ~20%

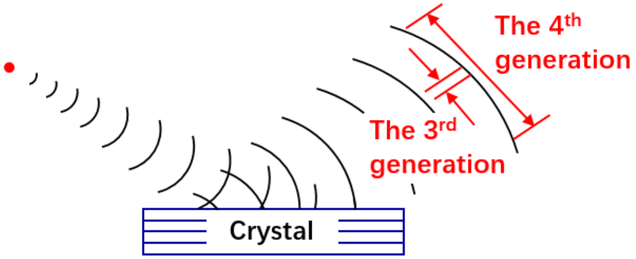


⇨ **Preserve wavefront in a much larger range**

**Unprecedented challenge to both crystal processing & diffraction wavefront measurement**

# Background

## ➢ Difficulties of crystal Bragg diffraction wavefront measurement

**Predominate wavefront measurement methods:**

**Speckle based wavefront metrology**

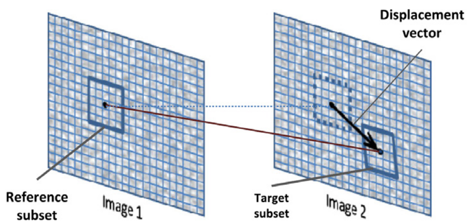


**Grating based wavefront metrology**

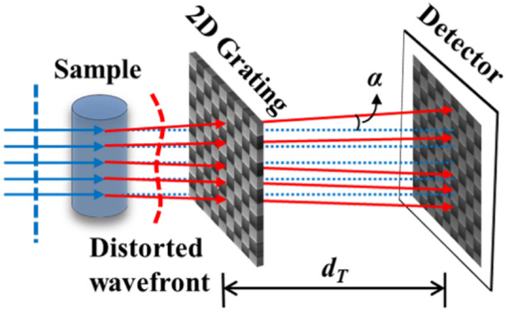


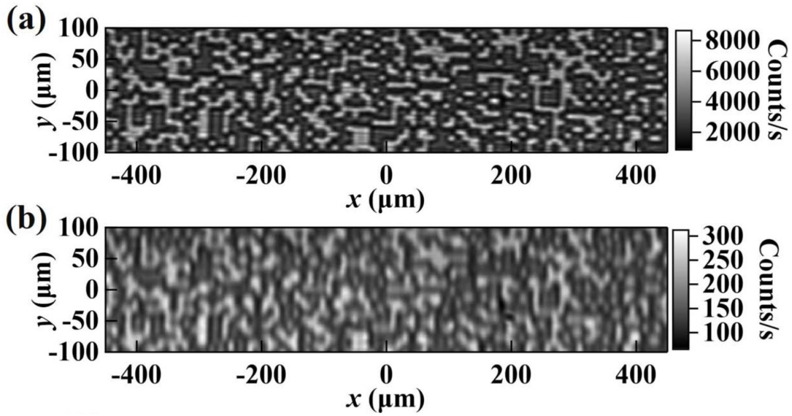


**Direct-beam**

**Diffracted-beam**

Crystal extinction effect

**Diffraction image blurred**

**①Large phase-detection errors**

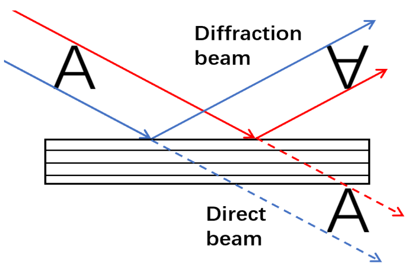


**②Beam flip for flat crystal**

Bérujon S., Ziegler E., Cerbino R., *et al. Physical Review Letters,* 2012, 108, 158102.
Shi X., Grizolli W., Shu D., *et al. Advances in Metrology for X-Ray and EUV Optics VIII*, 2019, 11109(111090K): 1-8.
Shi, X., Qiao, Z., Pradhan, P., *et al. Journal of Synchrotron Radiation,* 2023, 30, 1100-1107.

# The Double-edge Scan (DES) Method

## ➢ Methods introduction

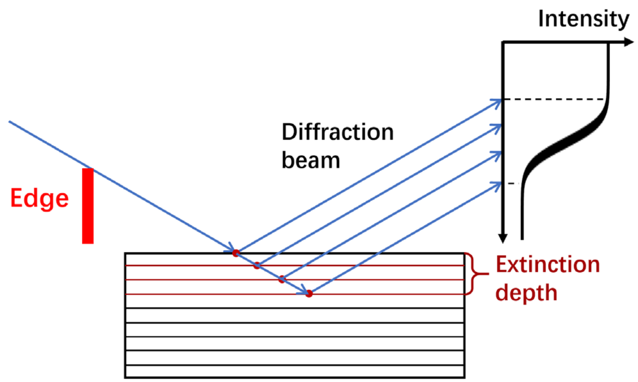


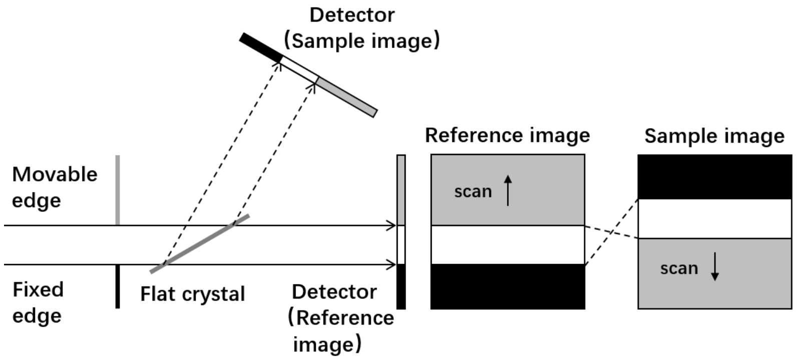


- **Use edges to track the beam deflection;**
- Image blurring **only broadening the edge projection;**
- **Hardly affect the positioning accuracy of a single edge projection;**
- **Based on geometric optics, not limited by transverse coherence.**

- **Use a fixed edge as a mark** when beam flipped;
- The **distortion of reference wavefront can be deducted**, the absolute diffraction wavefront can be measured.

**To be published**

# The Double-edge Scan (DES) Method

- **Methods introduction**

## The double-edge scan method:

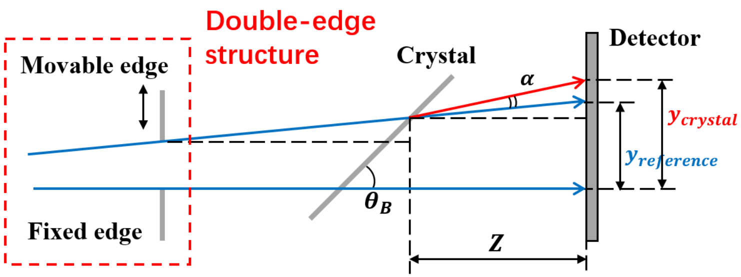


Diffraction wavefront slope error:

$$\alpha = \frac{y_{crystal} - y_{reference}}{Z}$$

## The pencil beam method:

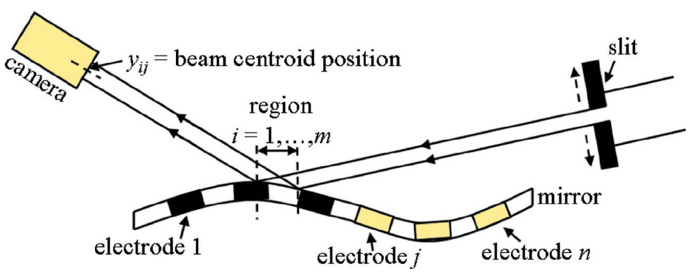


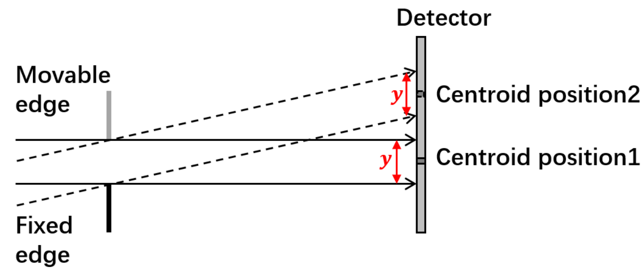


Measure the **distance *y* between the two edge projections** instead of the absolute centroid position**;**

**Exclude the influence of source instability.**

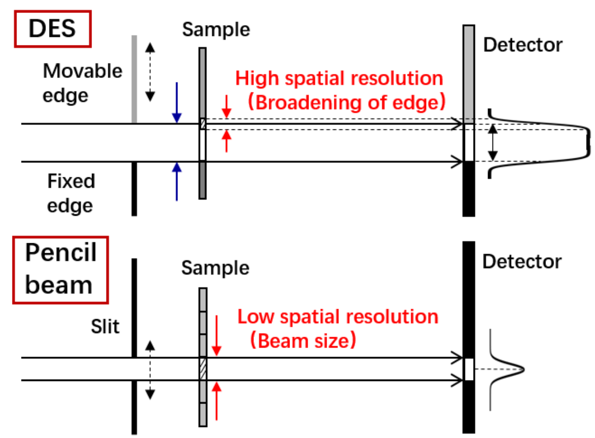


**High spatial Resolution;**

**High X-ray flux**

**To be published**

Sutter J., Alcock S., and Sawhney K., *Journal of Synchrotron Radiation*, 2012, 19, 960-968.

# The Double-edge Scan (DES) Method

## ➢ Experimental Setup

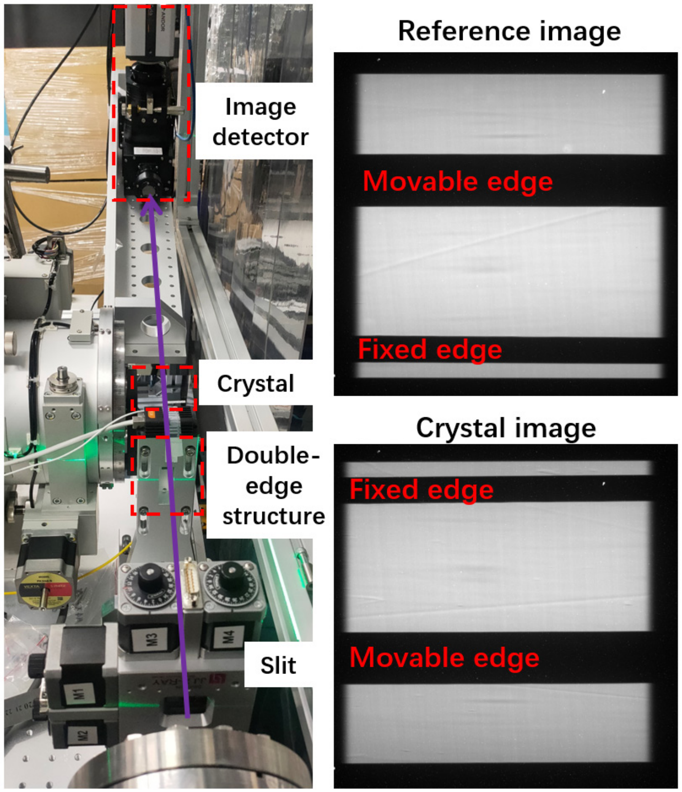


**Beijing Synchrotron Radiation Facility （1B3B)**
**1GSR**

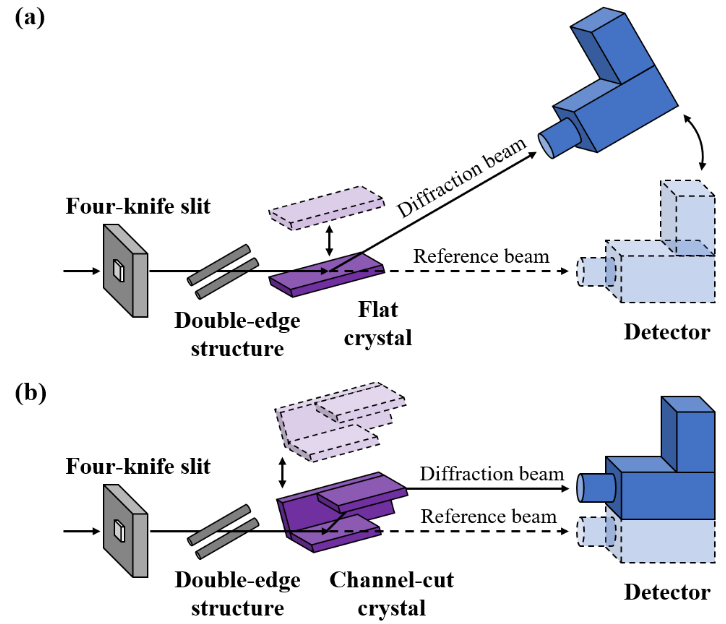


- Schematic (a) for flat crystal measurement;
- Schematic (b) for channel-cut crystal measurement;
- Energy: 15keV.

**To be published**

# Wavefront Measurement Results

- Self processed high quality flat crystal
- Self processed high quality channel-cut crystal
- Repeatability measurement
- Mirror slope error measurement

# Diffraction Wavefront Measurement

➢ **Flat crystal & Channel-cut crystal**

**Self processed flat crystal:**

Scanning step size ~**18 µm** in the wavefront coordinate:

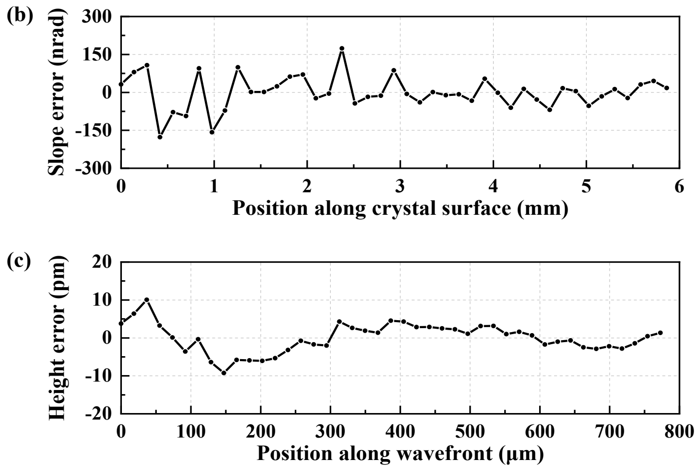


- Equivalent diffraction surface slope error: 65.91 nrad RMS;
- Wavefront height error: 3.78 pm RMS (or 4.57%λ **< λ/14**);
- **Meet the wavefront preservation requirement of the diffraction-limited sources.**

**Self processed channel-cut ctystal:**

Scanning step size ~**17 µm** in the wavefront coordinate:

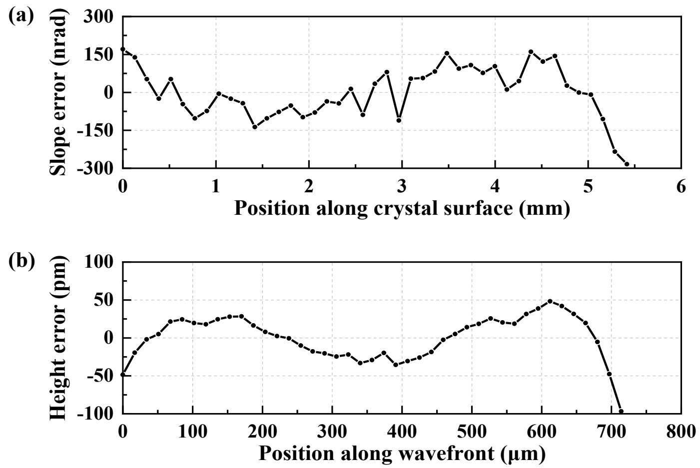


- Equivalent Bragg diffraction surface slope error: 101.73 nrad RMS;
- Wavefront height error: 7.65 pm RMS (or 9.25%λ) .
- Processing is much more difficult.

**To be published**

# Diffraction Wavefront Measurement

➢ **Repeatability measurement (Advantage of the double-edge structure)**

## Double edge mode:

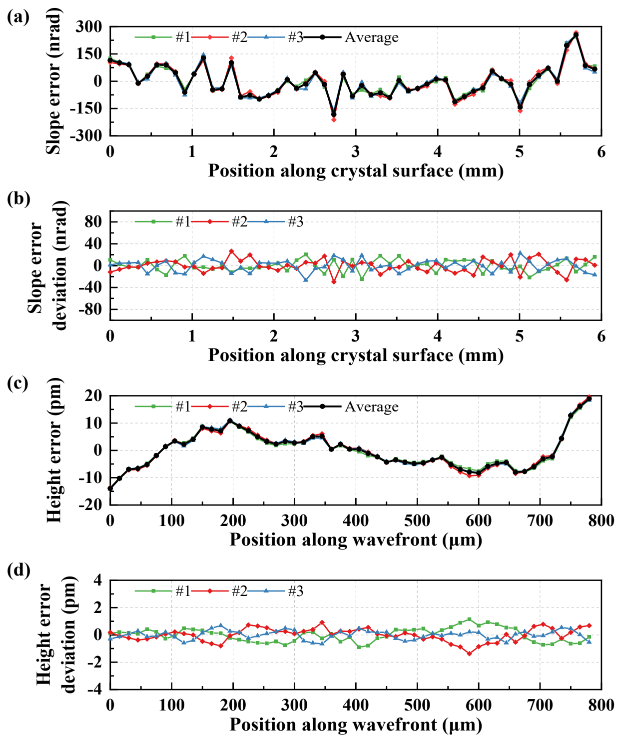


Average slope errors: 82.08 nrad RMS

**Repeatability: 13.51 nrad RMS** →

Average wavefront height error: 6.71 pm RMS

**Repeatability: 0.54 pm RMS** →

## Single edge mode:

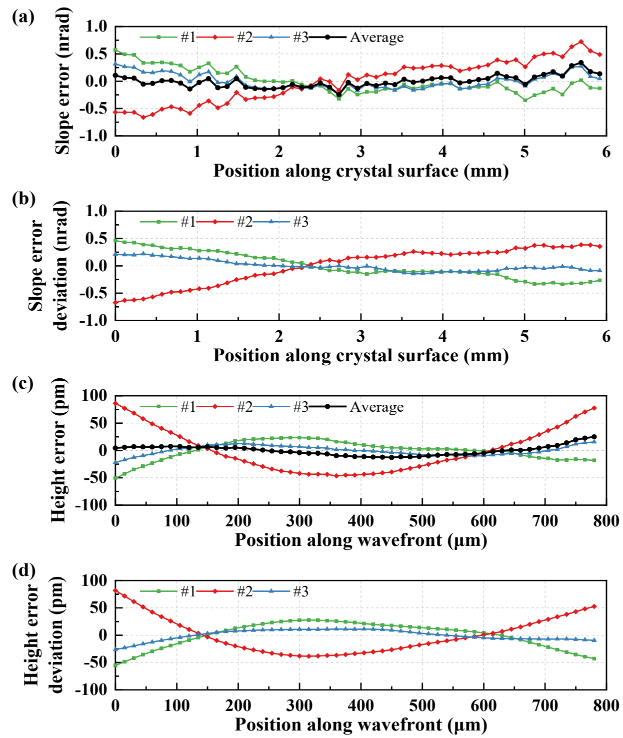


Average slope errors: 109.99 nrad RMS

**Repeatability: 296.33 nrad RMS**

Average wavefront height error: 8.94 pm RMS

**Repeatability: 28.99 pm RMS**

**Double-edge structure**

⇩

**Reduce repetitive measurement error**

**Improve reliability**

**To be published**

# Mirror Slope Error Measurement

- **Comparison with FSP (self developed long trace profiler)**

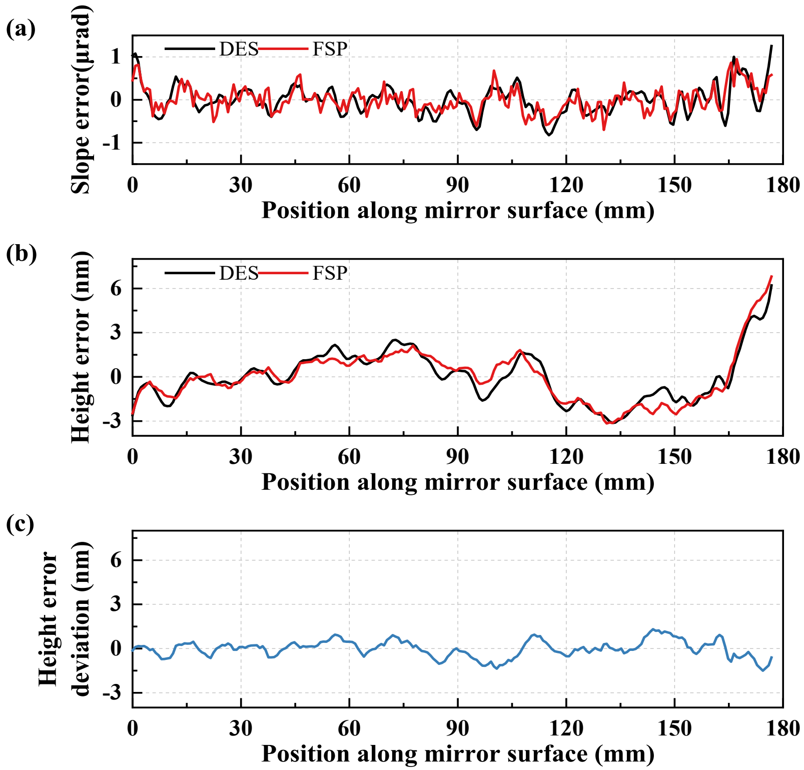


**Slope errors RMS:** 0.294 μrad (DES)

0.344 μrad (FSP)

**Height errors RMS:** 1.69 nm (DES)

1.76 nm (FSP)

**Height error deviations** between the two methods: 0.57 nm RMS

**The good agreement between the DES and the FSP method;**
**Is a noticeable progression which can strongly support the new DES method.**

**To be published**

# Magnetically-Controlled Chemical-Mechanical Polishing (MC-CMP)

- **Method introduction**
- **Other crystal characterized results**

# MC-CMP Method Introduction

## ➢ MC-CMP( Magnetically-Controlled Chemical-Mechanical Polishing)

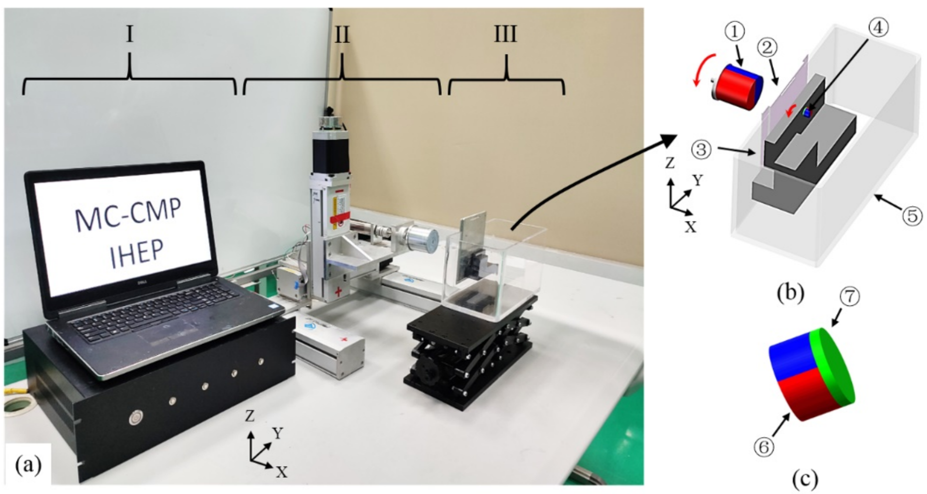


FIG.1. (a) photo of the MC-CMP system; (b) sketch of the vessel and a work piece of crystal and (c) Small polishing magnets. Major components are: ①large magnet ②the pad which can be inserted into the vessel; ③the channel-cut crystal; ④small polishing tool; ⑤vessel filled with slurry; ⑥mini magnet; ⑦covering layer

The Magnetically-controlled chemical-mechanical polishing (MC-CMP) system as shown in FIG.1 consists of three major components: a) a mini cylinder magnet in the vessel filled with slurry or polishing solution; b) a gantry guide rail and rotating mechanics for driving magnet; and c) a control computer. The rotation of the large cylinder magnet is achieved by a DC motor while the three-dimensional translation movements X/Y/Z movements are implemented through a gantry guide rail. Both magnets are radially magnetized.

## ➢ Advantages

a) **The stress can be automatically controlled by varying the distance along X-axis;**
b) **Owing to the small polishing magnets, it is highly feasible to fabricate channel-cut crystals with small gap;**
c) **With rotating and rectilinear motion, the processing path is complex which is benefit for the smoothing of inner surfaces;**
d) **High cost-effectiveness ratio;**

Hong, Z., Diao, Q., Xu, W., Yuan, Q., Yang, J., Li, Z., Jiang, Y., Zhang, C., Zhang, D., Liu, F., Zhang, X., Liu, P., Tao, Y., Sheng, W., Li, M. & Zhao, Y. (2023). *Journal of Synchrotron Radiation,* 30, 84-89.

# Fabrication of Channel-cut Crystal

## ☐ The design of CC crystal and small tool

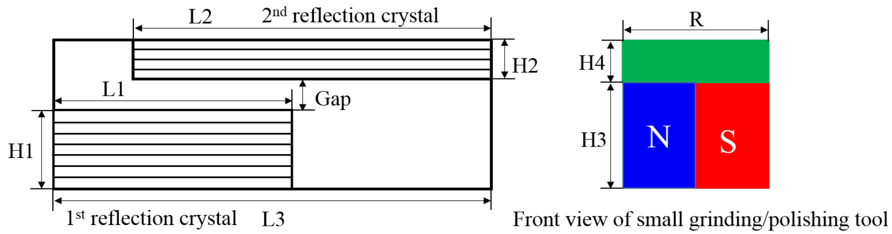


FIG.2 (left) Top view of the channel-cut crystal; (right) Front view of magnetic polishing tool; the size as indicated are listed in Table 1

Table 1 Dimensions as specified in Fig.2

| Dimension | L1 | L2 | L3 | H1 | H2 | Gap | H3 | H4 | R |
|---|---|---|---|---|---|---|---|---|---|
| Size(mm) | 60 | 90 | 110 | 20 | 10 | 7 | 4 | 2 | 8 |

## ☐ The processing path

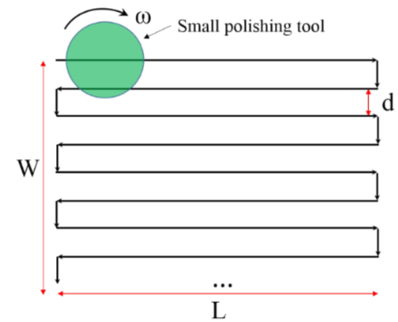


FIG.3. Scanning processing routes, where L, W and d refers to length, width and distance, respectively and ω is the rotation speed

## ☐ The force between small tool and crystal

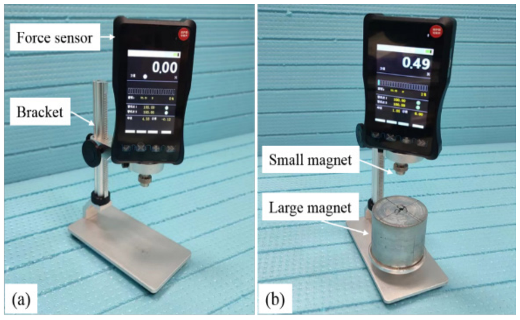


FIG.4. Picture of force measurement setup (a) Setting the force sensor to zero after small magnet amounted on; (b) Putting the large magnet under the small magnet.

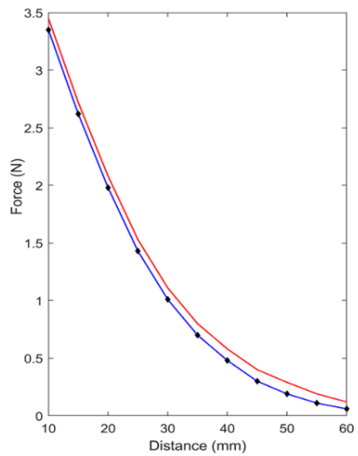


FIG.5. The relationship between the forces and distances of magnets

The distance dependent magnetic forces were measured using the experimental setup, shown in FIG.4. The small magnet was amounted on the trigger rod of force sensor which was placed on the aluminum bracket. The black points the blue solid line is the fitting curve of those points, the red solid is derived from Comsol Multiphysics 5.4.. **The variation trends are same, so the results are credible for the two measurement methods.** However simulated force values are slightly higher than the measured value. This might be due to the simplified model used in the simulation or the uncertainty of the measured value.

# Fabrication of Channel-cut Crystal

## The removal function

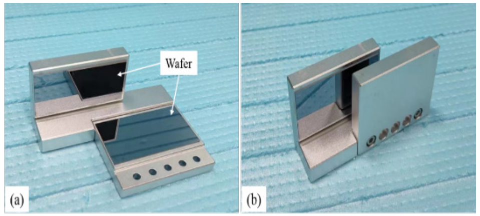


FIG.6. (a) photo of 'channel-cut crystal' made of aluminum; (b) 'channel-cut' after assembly

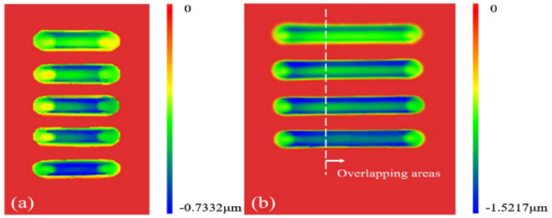


FIG.7. Removal footprints of polished silicon surface

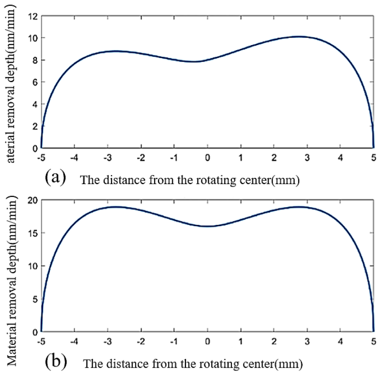


FIG.8. Removal function cutting line 'M' likeness (a) rotating& unidirectional direction linear movement (b) rotating & advance and return movement

A structure made of aluminum alloy was designed to perform optical metrology during processing, The relationship between volume removal rates and processing parameters (i.e. speed, distance) is experimentally determined, **the material removal is estimated by the relationship (removal function).**

## The processed CC crystal

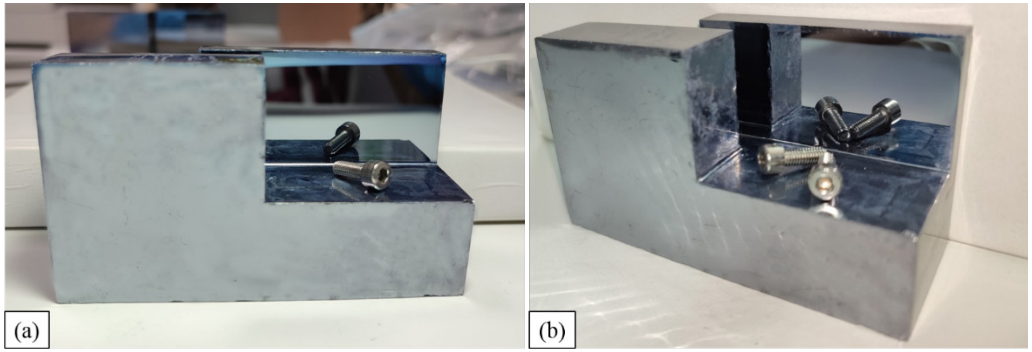


FIG.9. Photo of channel-cut crystal after MC-CMP polishing (a) front view; (b) side view; the screws are mirrored clearly by the polished mirror-like surface of the channel-cut crystal

## Processing Procedure

1) **Rough mechanical polishing. nearly 120μm-thick layer were removed.**
2) **Rough CMP polishing. a thickness ~55μm were removed.**
3) **Wet chemical etching (WCE).** The CC crystal was etched in $HNO_3$/HF (10:1) over 12 minutes. In this step, **totally 35-μm thick layer was removed.**
4) **Final CMP polishing.** Covering layer on the small tool was polyurethane, **nearly 8μm thickness was removed during polishing.**

# Experiments for Characterization

## ☐ Off-line characterization

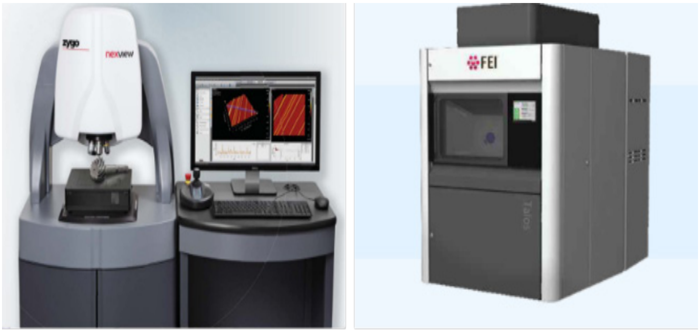

(a) (b)

FIG.10. (a) White light profilometer (b) Transmission electron microscope

To characterize the **details of surface and micro-structural changes of the material**, we carried out two optical investigations using the White Light Profiler (WLP, type: ZYGO SER 4405A) and the High Resolution Transmission Electron Microscopy (HR-TEM, type: FEI Talos F200x), respectively.

## ☐ On-line measurement

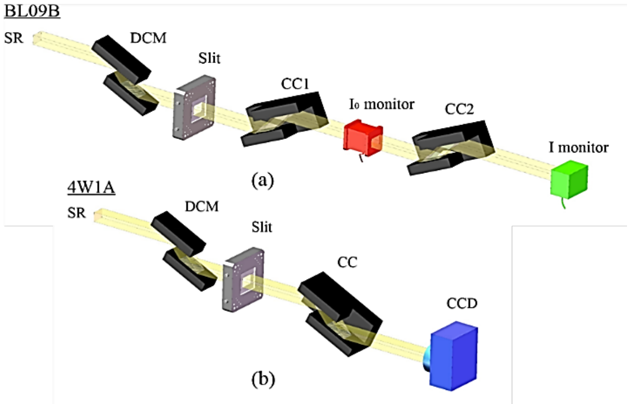


FIG.11. Schematic view of experiment setup for (a) Rocking-curve and reflectivity at BL09B, SSRF and 1B3B, BSRF

**The rocking curve and reflectivity was measured at the BL09B, Shanghai Synchrotron Radiation Facility (SSRF).** In this experiment (FIG.11(a)), the (+, −, −, +,−, + ) crystal configurations were adopted with double flat crystals and a pair of CC crystals**. The X-ray topography experiment was conducted at 4W1A, Beijing Synchrotron Radiation Facility (BSRF).** In this experiment (FIG.11(b)), the (+, − , +, − ) configuration was adopted. Both beamlines were equipped double crystal monochromator Si(111).

# Results & Discussion

## Roughness

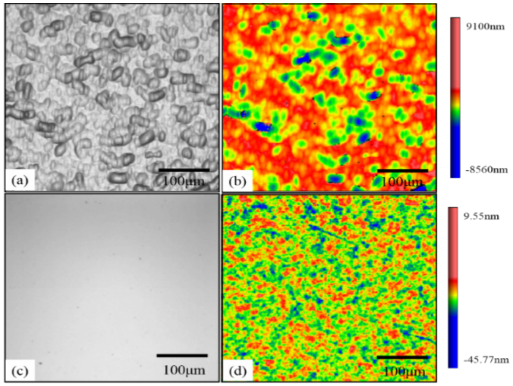


FIG.12. (a) Optical micrograph of WCE CC; (b) the corresponding roughness; (c) Optical micrograph of MC-CMP CC (d) the roughness.

For the channel-cut crystal with wet chemical etching (WCE), numerous and large-size speckles was found on the surface (FIG.12a) and the roughness value of the etched one is 873.9nm rms (FIG.12b). By contrast, for the MC-CMP channel-cut crystal, **the obtained surface is homogeneous without any observable speckle and scratch** (FIG.12c) and a substantially high surface roughness was measured as **0.614 nm** RMS (FIG.12d).

## Rocking-curve

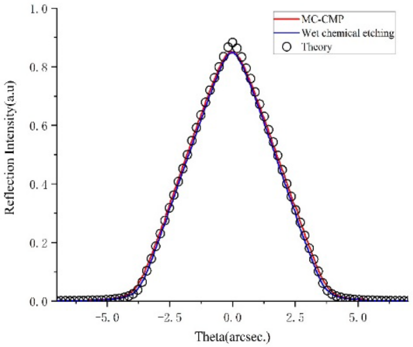


FIG.13. Comparison of experimental and theoretical rocking curves for MC-CMP and WCE processed channel-cut crystals.

The rocking curves at 15 keV was measured for both WCE CC and MC-CMP CC crystals. The **Darwin width** for both WCE and MC-CMP CC crystals **agrees well with the theoretical calculations** based on dynamical diffraction theory. Meanwhile, the peak **reflectivity** of MC-CMP CC and WCE CC are **85.1%** and 84.8% respectively, which are **close to theoretical value** of 88.3%. **Indicating that diffraction volume is perfect crystal and damaged layers are removed by both MC-CMP or WCE process. On the other hand, the diffraction surface is well preserved by using MC-CMP method for polishing the inner-face of channel-cut crystals.**

# Results & Discussion

## ❑ Topography

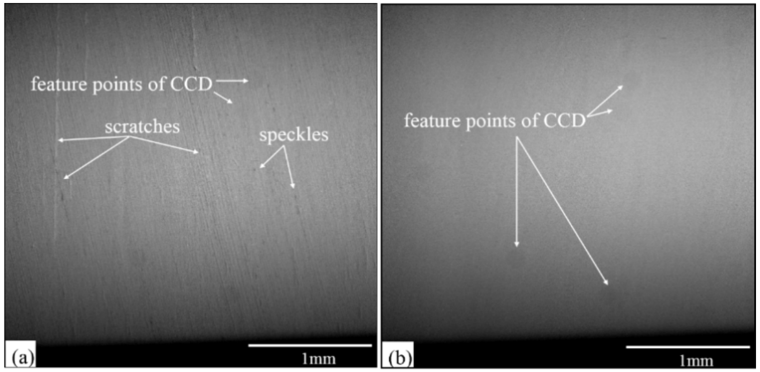


FIG.14. (a) Topography of etching surface (b) Topography of polishing surface

FIG.14. shows the X-ray topography of crystal surface for the WCE-CC and MC-CMP-CC crystals. There are numerous scratches in the WCE-CC crystals, but **the MC-CMP-CC crystal was quite homogeneous and free of scratch**. a few dark points originates from the CCD.

## ❑ HRTEM photograph and EDX mapping

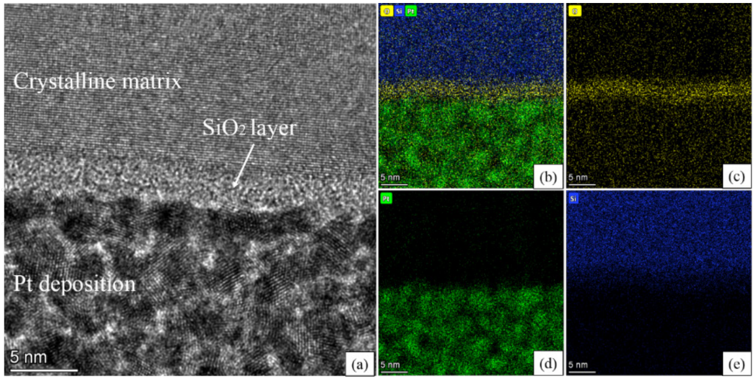


FIG.15. Cross section HRTEM photograph of polishing CC workpiece

According to the EDX mapping, a $SiO_2$ layer with a uniform thickness of about 2.5nm was found on the surface of the perfect crystalline matrix. There is no amorphous layers that often exist in the traditional CMP process, Using the MC-CMP method, **the $SiO_2$ layer (FIG.15) with nanometer scale thickness and uniform construction obtained on perfect crystalline matrix could be benefit to wavefront preserving and coherence of high quality photons from 4th generation synchrotron radiation or Free-electron lasers.**

# Conclusions

# Conclusions

1. **We developed the double-edges scan (DES) wavefront metrology method** at Beijing Synchrotron Radiation Facility (BSRF), and several vital problems of the 1st generation source had been resolved including **poor directional stability** of incident beam, **low X-ray flux** and **distortion of incident wavefront**.
2. **We have achieved diffraction-limit level crystal diffraction wavefront measurement**, the DES method has already been regarded as an important feedback in the next-generation crystal processing.
3. The measurement repeatability was below 15 nrad RMS, the diffraction wavefront slope error was below 70 nrad RMS for flat crystal and below 110 nrad RMS for channel-cut crystal.
4. The magnetically controlled Chemical Mechanical polishing **(MC-CMP) method is a nice approach with high cost-effectiveness ratio for polishing channel-cut crystals with small gap.**
5. We have attempted to process a mini-CC with ~800μm gap, the inner faces were improved significantly, detail measurement will carried out in the future.

**To be published**

# Thank you!

fliu@ihep.ac.cn;   hongzhen@ihep.ac.cn